Crystal Structure of Plasmodium falciparum Spermidine Synthase in Complex with the Substrate Decarboxylated S-adenosylmethionine and the Potent Inhibitors 4MCHA and AdoDATO

ARTICLE *in* JOURNAL OF MOLECULAR BIOLOGY · NOVEMBER 2007

Impact Factor: 4.33 · DOI: 10.1016/j.jmb.2007.07.053 · Source: PubMed

6 AUTHORS, INCLUDING:

Wei Qiu
AbbVie
35 PUBLICATIONS **1,023** CITATIONS
SEE PROFILE

Ingrid B Müller
Swiss Federal Institute of Intellectual Prop…
41 PUBLICATIONS **597** CITATIONS
SEE PROFILE

Raymond Hui
University of Toronto
48 PUBLICATIONS **1,891** CITATIONS
SEE PROFILE

Salam Al-Karadaghi
Lund University
70 PUBLICATIONS **2,156** CITATIONS
SEE PROFILE

doi:10.1016/j.jmb.2007.07.053 *J. Mol. Biol.* (2007) **373**, 167–177

JMB

Available online at www.sciencedirect.com

ScienceDirect

ELSEVIER

Crystal Structure of *Plasmodium falciparum* Spermidine Synthase in Complex with the Substrate Decarboxylated *S*-adenosylmethionine and the Potent Inhibitors 4MCHA and AdoDATO

Veronica Tamu Dufe[1]†, Wei Qiu[2]*†, Ingrid B. Müller[3], Raymond Hui[2], Rolf D. Walter[3] and Salam Al-Karadaghi[1]*

[1]*Department of Molecular Biophysics, Center for Molecular Protein Science, Lund University, Box 124, S-221 00 Lund, Sweden*

[2]*Structural Genomics Consortium, Banting Building, University of Toronto, 100 College Street, Toronto, ON, Canada M5G 1L5*

[3]*Department of Biochemistry, Bernhard Nocht Institute for Tropical Medicine, Hamburg, Germany*

Received 18 April 2007; received in revised form 11 July 2007; accepted 21 July 2007
Available online 2 August 2007

Edited by G. Schulz

Plasmodium falciparum is the causative agent of the most severe type of malaria, a life-threatening disease affecting the lives of over three billion people. Factors like widespread resistance against available drugs and absence of an effective vaccine are seriously compounding control of the malaria parasite. Thus, there is an urgent need for the identification and validation of new drug targets. The enzymes of the polyamine biosynthesis pathway have been suggested as possible targets for the treatment of malaria. One of these enzymes is spermidine synthase (SPDS, putrescine aminopropyltransferase), which catalyzes the transfer of an aminopropyl moiety from decarboxylated *S*-adenosylmethionine (dcAdoMet) to putrescine, leading to the formation of spermidine and 5′-methylthioadenosine. Here we present the three-dimensional structure of *P. falciparum* spermidine synthase (pfSPDS) in apo form, in complex with dcAdoMet and two inhibitors, *S*-adenosyl-1,8-diamino-3-thio-octane (AdoDATO) and *trans*-4-methylcyclohexylamine (4MCHA). The results show that binding of dcAdoMet to pfSPDS stabilizes the conformation of the flexible gatekeeper loop of the enzyme and affects the conformation of the active-site amino acid residues, preparing the protein for binding of the second substrate. The complexes of AdoDATO and 4MCHA with pfSPDS reveal the mode of interactions of these compounds with the enzyme. While AdoDATO essentially fills the entire active-site pocket, 4MCHA only occupies part of it, which suggests that simple modifications of this compound may yield more potent inhibitors of pfSPDS.

Keywords: malaria; inhibitor design; enzyme inhibition; polyamine synthesis; spermidine synthase

Introduction

Malaria is a life-threatening parasitic disease transmitted by female *Anopheles* mosquitoes. There are four types of human malaria parasites: *Plasmodium vivax*, *Plasmodium malariae*, *Plasmodium ovale* and *Plasmodium falciparum*, the last one being the causative agent of the most severe malaria. Over three billion people live under the threat of the disease and over a million (mostly children) die each year‡. Factors such as widespread resistance against

**Corresponding authors.* E-mail addresses: wei.qiu@utoronto.ca; salam.al-karadaghi@mbfys.lu.se.

† V.T.D. and W.Q. contributed equally to the work.

Abbreviations used: AdoDATO, *S*-adenosyl-1,8-diamino-3-thio-octane; AdoMetDC, *S*-adenosylmethionine decarboxylase; dcAdoMet, *S*-adenosylmethionine; 4MCHA, 4-methylcyclohexylamine; MTA, 5′-methylthioadenosine; ODC, ornithine decarboxylase; PAO, polyamine oxidase; SPDS, spermidine synthase; SPMS, spermine synthase; SSAT, N1-acetyltransferase.

‡ www.rollbackmalaria/wmr2005

available drugs and absence of an effective vaccine are seriously compounding control of the malaria parasite. Thus, there is an urgent need for the identification and validation of new drug targets. Based on the critical role of polyamines in key processes such as cell growth, differentiation and macromolecular synthesis, the enzymes of the polyamine biosynthesis pathway were suggested as targets in the treatment of parasitic diseases.[1–7] Additional support for this suggestion was obtained when it was shown that 2-difluoromethylornithine could successfully be used in the treatment of African sleeping sickness caused by *Trypanosoma brucei gambiense*.[7–10] 2-Difluoromethylornithine, which is an inhibitor of ornithine decarboxylase (ODC), the first committed enzyme in the polyamine biosynthesis pathway, has also been demonstrated to have limited activity against other parasitic protozoa, among which are *P. falciparum*, *Plasmodium berghei* and *Leishmania donovani*, the causative agent of leishmaniasis.[11–13]

The enzymes involved in the polyamine biosynthesis pathway include, together with ODC, *S*-adenosylmethionine decarboxylase (AdoMetDC), spermidine synthase (SPDS, putrescine aminopropyltransferase), spermine synthase (SPMS), spermidine/spermine N1-acetyltransferase (SSAT) and FAD-dependent polyamine oxidase (PAO). ODC produces putrescine by decarboxylation of ornithine. Putrescine in turn accepts an aminopropyl group to form spermidine in a reaction catalyzed by SPDS. The second product of the SPDS reaction is 5′-methylthioadenosine (MTA). The aminopropyl group is donated to putrescine by decarboxylated *S*-adenosylmethionine (dcAdoMet), which is the product of AdoMetDC. SSAT and PAO are involved in the conversion of spermidine and spermine to putrescine.

In comparison with mammalian cells, the polyamine biosynthesis pathway in *P. falciparum* is simpler, since no SPMS, SSAT and PAO enzyme activities, and subsequently no conversion from spermine and spermidine to putrescine, have been detected.[7] This makes the remaining enzymes of the pathway crucial for the survival of the parasite. One of these enzymes, suggested as a target in the treatment of *P. falciparum* infections, is SPDS.[14,15] Using null mutants, SPDS was also shown to be essential for the survival of *L. donovani*.[16] Among the first potent and selective inhibitors of SPDS was *S*-adenosyl-1,8-diamino-3-thio-octane (AdoDATO), a multisubstrate transition-state analogue that was already demonstrated in early studies to have an inhibitory effect on mammalian, trypanosomal and bacterial SPDS with an IC_{50} value of around 50 nM.[15,17] Another compound, *trans*-4-methylcyclohexylamine (4MCHA) was also demonstrated to inhibit rat SPDS with IC_{50} of about 1.7 μM.[18] The molecule was suggested to occupy part of the putrescine binding cavity and an adjacent hydrophobic region in the active site.[15,18] 4MCHA was also demonstrated to block development of *P. falciparum* (IC_{50} of 35 μM) and exhibit plasmodicidal activity.[19] An advantage of cyclohexylamine-based inhibitors was that they did not have the same adverse effects on mammalian cells as on malaria cultures.[20,21] Given that spermidine is required for the activation of the eukaryotic translation initiation factor eIF-5A and in trypanosomes for the biosynthesis of the glutathione mimic, trypanothione, the effects of SPDS inhibitors have been suggested to be attributed to the accumulation of unmodified eIF-5A in cells.[22–24]

SPDS from several sources have been crystallized and their structures solved by X-ray crystallography.[25–27] In order to get an insight into the structure–activity properties of *P. falciparum* SPDS (pfSPDS), in the present work we have determined the structure of the apo-pfSPDS as well as the structures of the complexes of pfSPDS with the substrate dcAdoMet and the inhibitors AdoDATO and 4MCHA.

Results

Overall structure of pfSPDS

A comparison of the amino acid sequences of SPDS from *P. falciparum* with the sequences of the enzyme from other organisms shows that pfSPDS possesses an N-terminal extension present only in some plants, among which is *Arabidopsis thaliana* SPDS[19] (Fig. 1). However, the N-terminal part of the sequence (29 amino acid residues) had to be omitted in order to get the expression of pfSPDS in *Escherichia coli*.[19] Crystallization efforts with this protein yielded only poor-quality crystals. Only further truncation of the sequence[28] up to residue 39 yielded better-quality crystals, which were used in this study.

pfSPDS expressed in *E. coli* was earlier reported to form a dimer in solution.[19] Most aminopropyltransferases that have been characterized are also homodimers, with the exception of those from thermophiles, which are tetramers.[14,25,26] pfSPDS used in the current study crystallized with three molecules per asymmetric unit. The interactions between the subunits were analyzed using the Protein–Protein Interactions Server§. The analysis showed that within the asymmetric unit, two of the molecules (B and C) interact with an interface burying around 1460 $Å^2$ of the total accessible surface area of each monomer, thus forming a dimer (Fig. 2a). On the other hand, the common surface between molecules A and B is only about 450 $Å^2$, which suggests non-specific crystal packing interactions.

The pfSPDS structure did not reveal any major deviation from the overall fold of *Thermotoga maritima* and *Caenorhabditis elegans* SPDS.[25,26] A comparison of the structures of apo-pfSPDS with the complexes of pfSPDS with dcAdoMet, dcAdoMet–4MCHA and AdoDATO gave rmsd values be-

§ http://www.biochem.ucl.ac.uk/bsm/PP/server

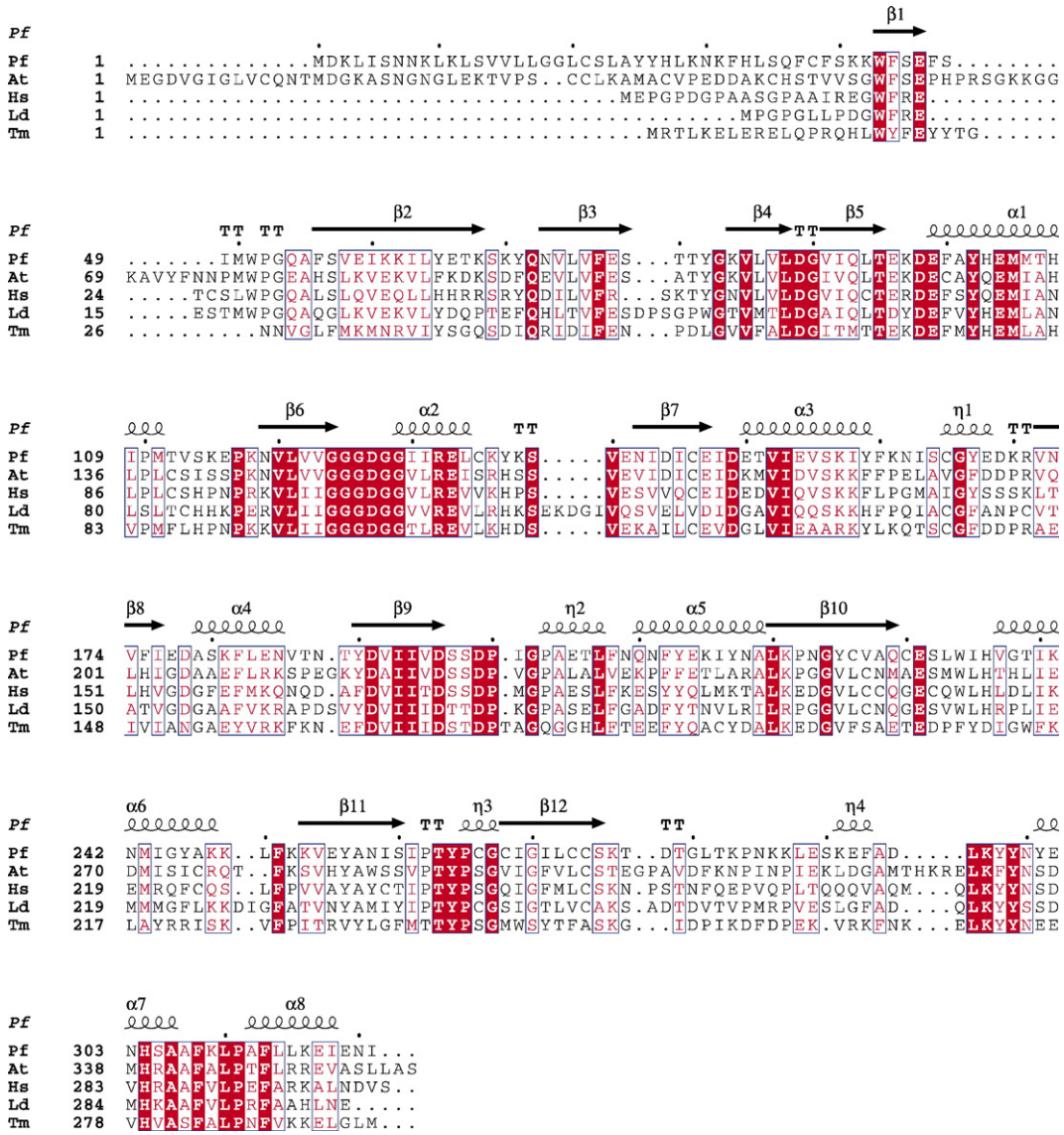

Fig. 1. Alignment of SPDS sequences from different organisms: Pf, *P. falciparum*, At, *A. thaliana*, Hs, *Homo sapiens*, Ld, *L. donovani*, Tm, *T. maritima*. Regions with conserved residues are boxed in blue with residues invariant in all organisms in red and conserved substitutions in white. The secondary structure elements for *P. falciparum* are shown above its sequence. TT = beta turn; η = helix turn; the dots show 10 residues apart in the *P. falciparum* sequence. For the secondary structure assignment the complex of pfSPDS with AdoDATO (PDB ID 2I7C) was used.

tween the C^{α} atoms of 0.37, 0.42 and 0.43 Å, respectively. Each monomer within the dimer consists of two domains: a small N-terminal domain and a large C-terminal domain (Fig. 2a). A five-stranded β-sheet builds up the N-terminal domain, which includes residues 41 to 97. Residues 98–321 build up the C-terminal catalytic domain, which includes a seven-stranded β-sheets and nine α-helices arranged in a Rossman-like fold. This topology, as reported earlier, has been found in other nucleotide and dinucleotide-binding enzymes, including *S*-adenosyl-L-methionine-dependent methyltransferases.[26] Apart from the residues omitted from the construct, 12 residues could not be modeled in each monomer of the apo structure. Most of these residues build up the so-called gatekeeper loop (residues 197–205), located between strand β9 and helix α5 (Fig. 2b). This loop was also reported to be disordered in the apo structures of *C. elegans* and *T. maritima* SPDS[25,26] and in the complex of human SPDS with MTA (PDB ID 1ZDZ). This loop is partially disordered in two of the molecules (A and B) in the asymmetric unit of the pfSPDS–MTA complex (PDB ID=2HTE). In contrast, it is well ordered and adopts almost the same conformation in the structures of the complexes of pfSPDS with AdoDATO, dcAdoMet and dcAdoMet–4MCHA (Fig. 2b). Two residues from this loop, the invariant D196 and P203, which are conserved in most organisms with the exception of *T. maritima* (Fig. 1), contribute to the interactions with dcAdoMet (Fig. 3a and b) and eventually to the stabilization of the loop conformation. Stabilization of the loop in the structure of the complex with dcAdoMet

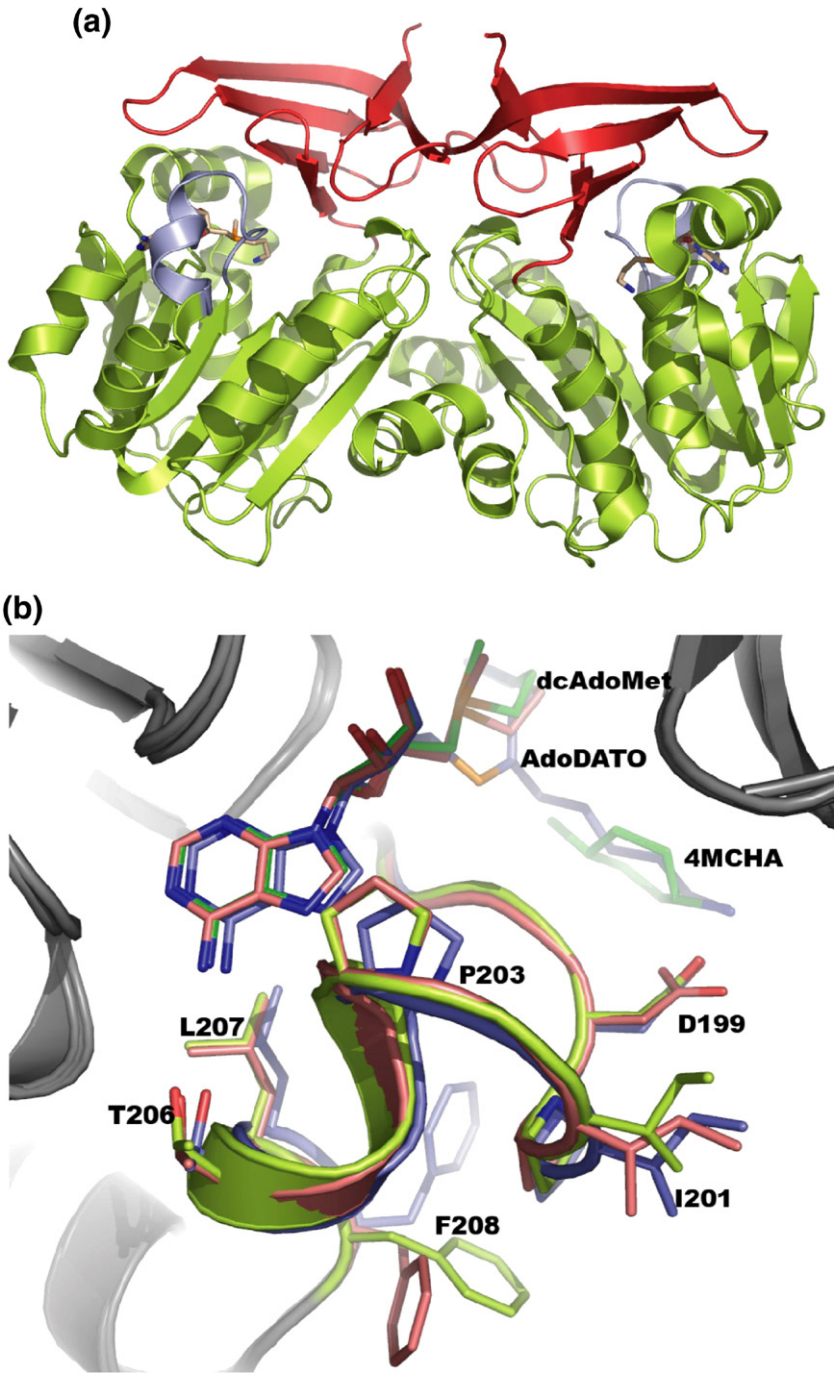

Fig. 2. The overall structure of pfSPDS. (a) A ribbon representation of the three-dimensional structure of *P. falciparum* SPDS. The N-terminal domain is red and the C-terminal domain is green. The gatekeeper loop is shown in light blue. The bound dcAdoMet is shown in stick representation to mark the position of the active site of the enzyme. (b) A superposition of the structures of the complexes of pfSPDS with AdoDATO (blue), dcAdoMet (orange) and dcAdoMet–4MCHA (green), showing the region of the gatekeeper loop. The only notable change is found in the conformation of the side chain of Phe208. Figures were prepared using Pymol.[40]

confirms earlier suggestions that it may act as a gatekeeper for the enzyme's active site.[26]

Binding of dcAdoMet and AdoDATO

The substrate dcAdoMet is bound in all three molecules in the asymmetric unit (Fig. 3a). Apart from the gatekeeper loop, which was mentioned above, there are some additional differences between the apo and dcAdoMet–pfSPDS complex structures. These include the region between strand β8 and a small helix α5 (residues 174–179). This loop moves closer to the adenosyl moiety, with a shift in the position of the C^{α} atom of the conserved D178 by approximately 1 Å. Also, the side chains of Q229 and the conserved Q93 and Y264 (Fig. 1), which are located close to the aminopropyl moiety, adopt different conformations in the structure of the complex (Fig. 3a). The conformations of these residues are the same in the complexes with dcAdoMet, AdoDATO and dcAdoMet–4MCHA, clearly suggesting that initial binding of dcAdoMet affects the conformation of the active-site environment, presumably preparing it for the binding of the second substrate. As will be shown below, without the addition of dcAdoMet no binding of the inhibitor 4MCHA could be observed in attempts to co-crystallize it with the enzyme. It should be noted that the comparison of the apo and AdoDATO complex structures of *T. maritima* SPDS (tmSPDS)

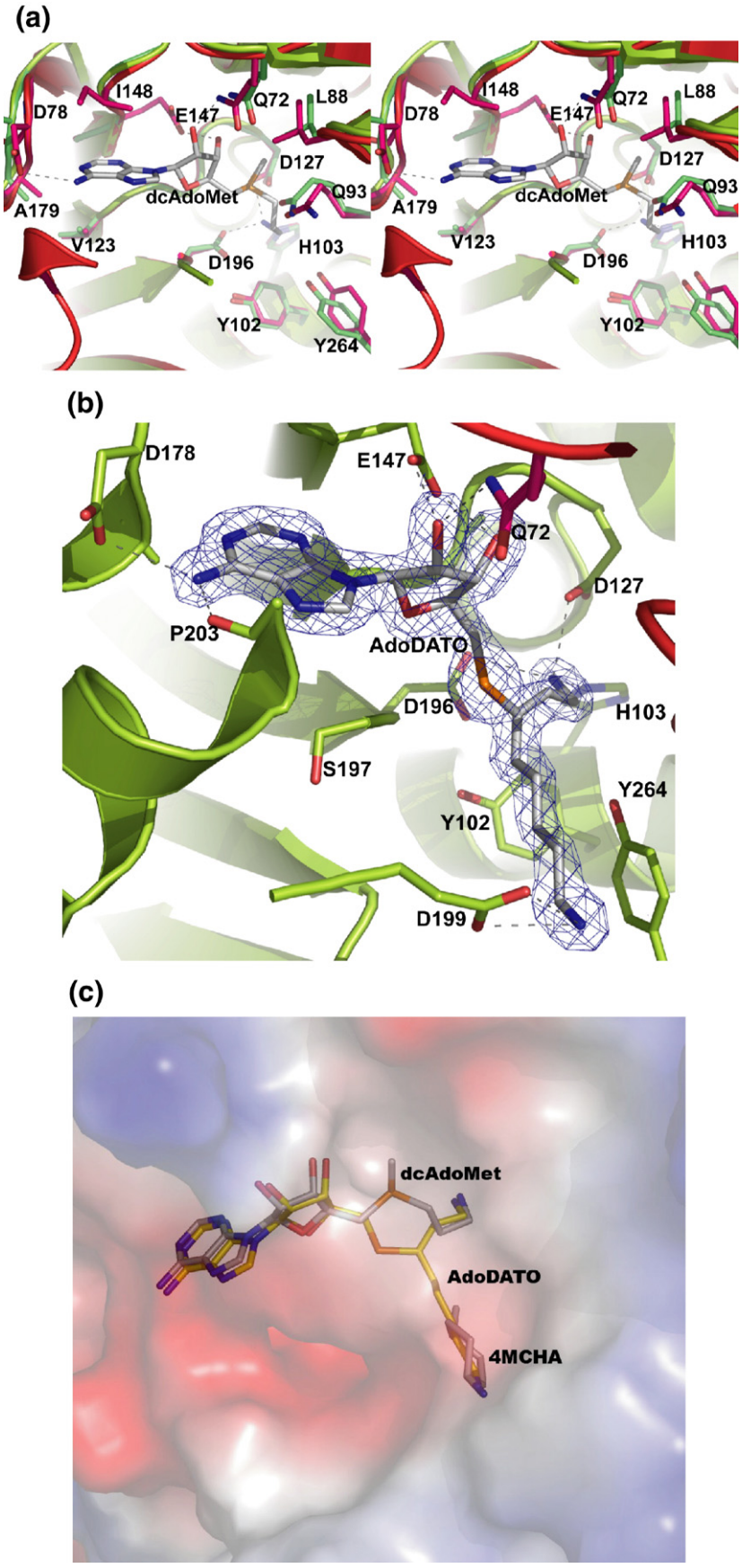

Fig. 3. dcAdoMet and AdoDATO binding to pfSPDS. (a) A stereo view showing a superposition of apo-pfSPDS (green) and the dcAdoMet complex (red). dcAdoMet and amino acid side chains that contribute to its binding are shown in stick representation: grey, blue, red and yellow represent carbon, nitrogen, oxygen and sulfur atoms, respectively. Dashed lines show hydrogen bonds. (b) Binding of AdoDATO to pfSPDS. The color scheme is as in (a). A $2F_o - F_c$ electron density map is shown superimposed on the inhibitor. (c) A superposition showing dcAdoMet, AdoDATO and 4MCHA. The sulfur atoms of dcAdoMet and AdoDATO occupy different positions. 4MCHA superimposes well on the putrescine moiety of AdoDATO. The protein is shown in surface representation, with red for regions of negative surface potential and blue for positive potential.

shows no differences in the conformation of the active-site residues.[26] This may be a result of the temperature of crystallization, which was far from the optimal temperature of growth of *T. maritima* (around 80 °C).

The coordinates of human SPDS in complex with dcAdoMet have recently been deposited in the PDB (Wu *et al.*, unpublished; PDB ID 2O0L). The binding of dcAdoMet shows features similar to those of the complex of dcAdoMet with pfSPDS.

The mode of dcAdoMet binding has been described earlier based on the crystal structure of the complex of tmSPDS with the transition-state analogue AdoDATO.[14,15,17] The adenosyl moiety of dcAdoMet in the present complexes superimposes on that of AdoDATO in complex with pfSPDS, with only a limited shift of 0.55 Å in the relative position of the two ligands (Fig. 3b and c). The side chain of D178 and the carbonyl oxygen of Pro203 form hydrogen bonds with the amine of the adenosyl groups of dcAdoMet and AdoDATO. Other conserved interactions between the two ligands and the protein include the side chains of E147 and Q72, which interact with the hydroxyls of the ribosyl moiety of dcAdoMet and AdoDATO (about 2.7 and 3.2 Å, respectively). As can be seen from the distances between the protein side chains and the ligands, no solvent molecules can be fitted into these positions to mediate the interactions, as was suggested by molecular dynamics simulations.[29] It is also seen from Fig. 3c that the sulfonic atom of AdoDATO has flipped to a position opposite to that of the sulfur of dcAdoMet. The methyl group linked to the sulfur atom of dcAdoMet binds in a pocket that is mostly hydrophobic (Fig. 3a). The aminopropyl chain of dcAdoMet interacts with the side chains of H103 and the invariant D127 and D196, which are located at approximately 2.7 and 2.9 Å, respectively, with slight differences in the different subunits. As suggested earlier, the position of the side chain of D196 is stabilized by interaction with Y102 (2.6 Å). It has been suggested that the role of H103, D127 and D196 is the proper orientation of the aminopropyl group and the carbon atom, which would allow for a nucleophilic attack by putrescine.[26]

AdoDATO specifically inhibits SPDS from various organism with an IC_{50} value in nano- to low micromolar range.[17] The IC_{50} for pfSPDS inhibition was determined to be 8.5±0.3 μM and is thereby only slightly higher than that reported for SPDS from other organisms. Overall, AdoDATO binding mode in pfSPDS is similar to the binding mode in the complex with tmSPDS.[26] A superposition of the structures of AdoDATO and dcAdoMet–4MCHA complexes shows that AdoDATO occupies the dcAdoMet and the putrescine binding pockets (Fig. 3c), with almost the same residues interacting with AdoDATO as with dcAdoMet and 4MCHA. Interestingly, a comparison of the complexes of MTA–pfSPDS (PDB ID 2HTE) and AdoDATO–pfSPDS shows that while MTA has essentially the same conformation and orientation as the adenosyl moiety of AdoDATO, the sulfide atom of MTA has two different positions. One of these (subunit C) is similar to the position of the sulfur atom of AdoDATO, while in the other two subunits (A and B) it is different. Since, as mentioned above, subunit C had a relatively ordered gatekeeper loop, while in subunits A and B it was disordered, this suggests that the sulfide group of MTA may affect the stability of the loop, facilitating the release of MTA from the active site of the enzyme. However, it cannot be excluded that the observed differences in the position of the sulfide atom of MTA depend on the crystallization conditions.

Binding of 4MCHA

As noted above, data collected from crystals of pfSPDS grown in the presence of 4MCHA alone did not show the inhibitor at the active site or at any other location in the structure. On the other hand, co-crystallization with the protein that was preincubated with dcAdoMet resulted in a complex with 4MCHA bound at the active site of all three molecules in the asymmetric unit. The substrate-binding pocket, as described earlier in tmSPDS, is hydrophobic in the central part and is occupied by acidic residues at both ends. The negative charge of the acidic residues contributes to the stabilization of the position of the amino groups of putrescine. The superposition of the structure of human SPDS in complex with putrescine and MTA (PDB ID=2O06) on the structure of the present complex shows that the positions of 4MCHA and putrescine are essentially the same (Fig. 4a and b). The cyclohexyl ring and the methyl group of 4MCHA align well with the methylene groups of putrescine, while the amine is aligned with the nonattacking nitrogen of putrescine. This mode of binding of 4MCHA is different from that suggested on the basis of docking studies.[29] The inhibitor appears to be primarily stabilized by a hydrogen bond between the side chain of the invariant D199 (D176 in human SPDS; Fig. 1) and the amine and by stacking of the cyclohexene ring against the side chain of the invariant Y264 (Y241 in human SPDS). Most notable is the rotation of the side chain of Y264 upon binding of 4MCHA: in the apo structure, the aromatic ring of the tyrosine is perpendicular to the cyclohexene plane (Fig. 3a). Two solvent molecules at 2.8 and 3 Å from the amine make hydrogen-bonding interactions with E231 and E46, respectively. These solvent molecules probably also contribute to the stabilization of the position of the inhibitor. Thus, the amine of 4MCHA occupies one of the negatively charged sites responsible for anchoring putrescine.[14,26] As seen from Fig. 4b, the methyl group of 4MCHA occupies the position of the methylene groups of putrescine. In order for this hydrophobic cavity to be accessible to the inhibitor, the side chains of Q93, Q229, Y264 and I269 need to adjust their position, which takes place after dcAdoMet binding (Fig. 3a). The analysis suggests that the methyl group, which is absent in cyclohexylamine,

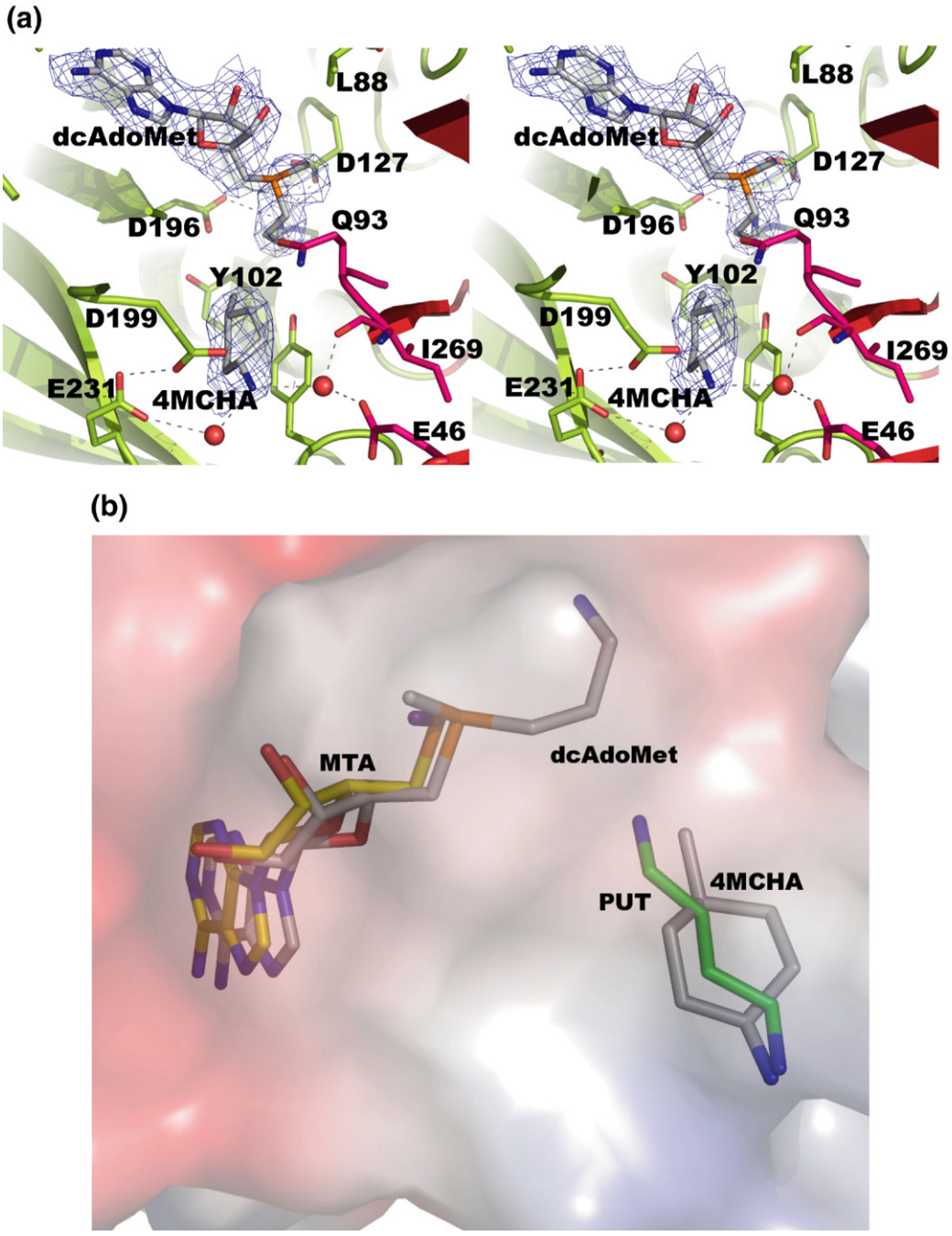

Fig. 4. The complex of 4MCHA–dcAdoMet with pfSPDS. (a) A stereo view showing the binding of 4MCHA and dcAdoMet. 4MCHA and amino acid side chains are shown in stick representation. The color scheme is similar to that of Fig. 3. Red spheres represent solvent molecules. An $F_o - F_c$ difference electron density map is shown covering the inhibitor and dcAdoMet (blue mesh). (b) A superposition of the structure of the 4MCHA–pfSPDS complex on the structure of human SPDS (PDB ID 2O06) in complex with MTA and putrescine (PUT).

most probably determines the relatively higher affinity of 4MCHA to SPDS. The second negatively charged pocket made up of the side chains of Y102, D196, Y264 and the backbone carbonyl of S197 is where the attacking amine of putrescine binds. This pocket is not occupied by 4MCHA and could probably be used in future modifications of the inhibitor aimed at development of new compounds with higher inhibitory capacity. Surprisingly, the electron density map of the model showed that the 4MCHA molecule was actually a *cis* rather than a *trans* 4-methylcyclohexylamine.

Discussion

Previous studies on polyamine metabolism in *Plasmodium* have been focused on ODC and AdoMetDC, which are known to have a key regulatory function within the polyamine biosynthesis path-

way. This also made them the primary target for research aimed at understanding the mechanisms of their function and inhibition. Prior to the biochemical characterization, relatively little attention has been given to SPDS from *P. falciparum*.[19]

An important feature of SPDS is the high conservation of the active site of the enzyme, although there are some differences in substrate specificity between different species.[26] Thus, human SPDS have been demonstrated to have high specificity towards putrescine, while pfSPDS, *E. coli* and *T. maritima* enzymes could produce small amounts of spermine, using spermidine as the aminopropyl group acceptor.[19,26,30] It has also been shown that pfSPDS had higher K_m for dcAdoMet (35 μM) than mammalian (7–25 μM), *E. coli* (2 μM) and plant enzymes (0.4–4 μM). This may explain the slightly elevated IC_{50} value for AdoDATO (8.5 μM) as compared to other organisms. It has been suggested that substrate specificity of SPDS may be affected by the gatekeeper loop, which contains the conserved aspartate (D199 in pfSPDS) that anchors the nonattacking amine group of putrescine.[14] Thus, in tmSPDS this loop appears to have greater flexibility because of an extra residue and a missing proline, which may facilitate the binding of polyamines other than putrescine.[14] The loop between β-strands β1 and β2 (F48-W51 in pfSPDS) has also been suggested to be involved in the closing of the active-site pocket, thus limiting the length of polyamine molecules that could bind to the enzyme.[14,26] A tryptophan (W51 in pfSPDS) serves in closing the active-site pocket at the side of the nonattacking amino group of the polyamine substrate. The promiscuous tmSPDS has a tyrosine at this position and one amino acid less in the loop, resulting in a larger cavity, which presumably enables the enzyme to bind longer chain diamines. A superposition of the human SPDS–MTA–putrescine and dcAdoMet–4MCHA–pfSPDS complex structures shows that this loop adopts a similar conformation, thus limiting the size of the putrescine-binding pocket. Since the gatekeeper loop also adopts a similar conformation in these two structures (Fig. 2b), it may appear that the putrescine-binding pocket of pfSPDS, like the human enzyme, does not have room to accommodate a longer chain polyamine like the triamine spermidine. However, there are some differences between the amino acid sequences of the loop in *P. falciparum* and the human enzymes, which include the substitutions Phe47Thr, Ser48Cys, Ile49Ser and Met50Leu (the first amino acid refers to pfSPDS). These substitutions may affect the flexibility of the loop in the case of pfSPDS, and thus allow the binding of longer chain polyamines, which would explain the limited SPMS activity observed for pfSPDS.[19] These differences may be utilized in future design of inhibitors with higher specificity towards the *Plasmodium* SPDS.

Our crystallization efforts demonstrated that dcAdoMet was needed in order for 4MCHA to bind. There were no indications of the protein being aminopropylated in the dcAdoMet complex structure, although *E. coli* and soybean axes SPDS have been suggested to carry out aminopropyl transfer through a ping-pong mechanism.[31,32] The requirement for dcAdomet for 4MCHA binding most probably means that for this two-substrate reaction, the two substrates must be added in a compulsory order. This observation also supports earlier suggestions that the reaction proceeds through an SN_2 path with the methylene carbon on dcAdoMet undergoing nucleophilic attack by the attacking nitrogen of putrescine.[14]

Materials and Methods

Cloning and expression

In an earlier work, recombinant expression in *E. coli* of the full-length pfSPDS was not successful.[19] When the first 29 amino acids were omitted, good quantity of expression of SPDS was achieved. However, attempts to get good-quality diffracting crystals from this protein did not succeed. Instead, the DNA sequence, corresponding to a protein lacking 39 residues at the N terminus, was synthesized and cloned into p15-Tev-LIC vector.[28] The protein was expressed in *E. coli* BL21-(DE3)-Rosetta Oxford in Terrific Broth in the presence of ampicillin/chloramphenicol (100 and 34 μg/ml, respectively). A single colony was inoculated into 100 ml of LB with of ampicillin/chloramphenicol (100 and 34 μg/ml, respectively) in a 250-ml baffled flask and incubated with shaking at 250 rpm overnight at 37 °C. The culture was transferred into 1.8 l of Terrific Broth with ampicillin/chloramphenicol (100 and 34 μg/ml, respectively) and 0.3 ml of antifoam (Sigma) in a 2-l bottle and cultured using the LEX system to an OD_{600} of 4.5.[28] Subsequently, it was cooled to 15 °C and induced with 0.5 mM IPTG overnight at 15 °C.

Protein purification

The culture was harvested by centrifugation. Pellets from 4 l of culture were resuspended to approximately 40 ml/l of cell culture in Binding Buffer [50 mM Hepes (pH 7.5), 500 mM NaCl, 5 mM imidazole and 5% glycerol] with the addition of protease inhibitors (1 mM benzamidine and 1 mM PMSF). Resuspended pellets stored at −80 °C were thawed overnight at 4 °C on the day before purification. Prior to mechanical lysis, each pellet from 1 l of culture was pretreated with 0.5% Chaps (3-[(3-cholamidopropyl)dimethylammonio]propanesulfonic acid) and 500 units of benzonase for 40 min at room temperature. Cells were mechanically lysed with a microfluidizer (Microfluidizer Processor, M-110EH) at approximately 16,000 psi, and the cell lysate was centrifuged using a Beckman JA-25.50 rotor at 24,000 rpm (~75,000*g*) for 20 min at 10 °C.

The buffer compositions were as follows: Elution Buffer: 50 mM Hepes (pH 7.5), 500 mM NaCl, 250 mM imidazole and 5% glycerol; Wash Buffer: 50 mM Hepes (pH 7.5), 500 mM NaCl, 30 mM imidazole and 5% glycerol; Crystal Buffer: 10 mM Hepes (pH 7.5), 500 mM NaCl. The cleared lysate was loaded onto a column prepacked with 10 g DE52 (Whatman) anion exchange resin (previously activated with 2.5 M NaCl and equilibrated with Binding Buffer). The DE52 column was further washed with 20 ml

Table 1. Data collection and refinement statistics

	Apo	dcAdoMet	dcAdoMet+4MCHA	AdoDATO
Data collection				
Resolution range (Å)	20.0–2.2	20.0–2.0	20.0–2.2	35.9–1.7
Completeness (%)[a]	94.3 (93.0)	96.1 (93.9)	96.2 (93.8)	94.0
Unique reflections	59,477	80,780	60,721	122,193
Multiplicity	2.3	3.2	3.5	3.7
$I/\sigma(I)$	11.6 (5.4)	13.7 (5.3)	10.1 (3.9)	25.7 (2.7)
R_{meas} (%)[b]	7.8 (25.2)	7.2 (26.9)	7.6 (25.4)	4.6 (32.2)
Refinement				
No. of protein atoms	6488	6773	6753	6849
No. of water molecules	275	412	202	589
dcAdoMet		3	3	
4MCHA			3	
AdoDATO				3
Glycerol	3	3	3	3
PEG	2	2	2	2
Sulfate ions	1		1	
R_{cryst} (R_{free})[c]	0.205 (0.247)	0.180 (0.214)	0.196 (0.239)	0.176 (0.194)
Mean *B*-factors (Å^2)	37	31	35	25
rmsd from ideality				
Bond lengths (Å)	0.013	0.012	0.013	0.013
Bond angles (°)	1.4	1.3	1.4	1.3
Chiral (°)	0.09	0.09	0.10	0.09
Ramachandran				
Core (%)	87.9	89.1	89.4	97.4
Allowed (%)	11.9	10.8	10.4	2.6
Disallowed (%)	0.3	0.1	0.1	0.0
PDB ID	2PSS	2PT6	2PT9	2I7C

R_{free} is the same as R_{cryst}, but calculated on 5% of the data excluded from refinement. Space group *C*2. Unit cell parameters for the apo-SPDS, dcAdoMet, dcAdoMet–4MCHA and AdoDATO complexes were 195.6, 134.2, and 48.4 Å, $\beta = 94.1°$; 196.3, 134.2, and 48.3 Å, $\beta = 94.4°$; 196.2 Å, 134.1 Å, 48.4 Å, $\beta = 94.5°$; 198.2 Å, 134.7 Å, 48.5 Å, $\beta = 95.4°$, respectively. All data, but the AdoDATO complex, were collected at Maxlab synchrotron source, station I911-2 (Lund, Sweden). The AdoDATO complex data were collected at APS 17-BM.

[a] The numbers in parentheses are for the highest resolution shell.

[b] $R_{merge} = \sum_i | I - \langle I \rangle | / \sum_i (I)$.

[c] $R_{cryst} = \sum | F_o - F_c | / \sum F_o$, where F_o and F_c are the observed and calculated structure factor amplitudes, respectively.

of Binding Buffer. The flow-through was subsequently loaded onto a 1.0- to 2.5-ml Ni-NTA (Qiagen) column (preequilibrated with Binding Buffer) at approximately 1–1.5 ml/min. The Ni-NTA column was then washed with 200 ml of Wash Buffer at 2–2.5 ml/min. After washing, the protein was eluted with 15 ml of Elution Buffer. EDTA was immediately added to the elution fraction to 1 mM, and DTT was added to 5 mM after approximately 15 more minutes. The eluted pfSPDS was applied to a Sephadex S200 26/60 gel filtration column preequilibrated with Crystal Buffer. The fractions corresponding to the eluted protein peak were collected. The His-tag was cleaved with TEV protease overnight at 4 °C in the presence of 1 mM DTT. The cleaved sample was applied to a 1-ml Ni-NTA column preequilibrated with Binding Buffer. The flow-through was collected, and the column was rinsed with an additional 5 ml of Binding Buffer. These fractions were pooled and concentrated using a 15-ml Amicon Ultra centrifugal filter device (Millipore). Using the same device, Binding Buffer was exchanged with Crystal Buffer by adding 15 ml Crystal Buffer twice to the portion of protein solution that was concentrated to around 0.5 ml. Finally, the protein was concentrated to 14.2 mg/ml and stored at −80 °C.

Crystallization, data collection and structure determination

Purified pfSPDS (14 mg/ml) was crystallized using the sitting drop vapor diffusion method at 15 °C. Protein solution (0.5 μl) was mixed with 0.5 μl of the reservoir solution containing 23% PEG3350, 0.1 M ammonium sulfate and 0.1 M Bis-Tris (pH 5.5). The pfSPDS–dcAdoMet complex was obtained by first incubating the protein with 2.5 mM dcAdoMet for 10 min at room temperature before mixing it with the reservoir solution. Protein–ligand solution (0.5 μl) was mixed with 0.5 μl of the reservoir solution containing 23% PEG3350, 0.1 M ammonium sulfate and 0.1 M Bis-Tris (pH 5.5). The pfSPDS–4MCHA–dcAdoMet complex was crystallized by incubating the protein already incubated with dcAdoMet with 2.5 mM 4MCHA for 10 min at room temperature. Protein–ligand solution (0.5 μl) was then mixed with 0.5 μl of the reservoir solution containing 23% PEG3350, 0.1 M ammonium sulfate and 0.1 M Bis-Tris (pH 5.5). The plates were then kept at 15 °C and single crystals appeared after 2 days in all setups. The AdoDATO complex was obtained by transferring pfSPDS–MTA crystals into 15% glycerol cryoprotectant solution containing 1 mM AdoDATO and incubating overnight‖.

Data were collected at beamline I911-2 (MAX Lab, Lund, Sweden) and APS Beamline 17-BM (Argonne National Laboratory, USA). The apo and complex crystals belonged to the same space group, *C*2, with three molecules in the asymmetric unit. Prior to data collection,

‖ The growth of the pfSPDS–MTA crystals is described at http://sgc.utoronto.ca/SGC-WebPages/StructureDescription/2HTE.php.

crystals were transferred to 25% glycerol for a few seconds before flash freezing in a boiled-off liquid nitrogen stream at 100 K. Data were processed using the XDS package.[33] The data quality was checked with the program TRUNCATE.[34] Molecular replacement program PHASER and the coordinates of the pfSPDS–AdoDATO complex (PDB ID 2I7C) with solvent and ligand molecules removed were used for obtaining the initial phases.[35] Coot and refmac5 were used for model building and refinement, respectively.[36,37] The library files of the ligands were generated by the PRODRG2 server.[38] Model quality was checked with PROCHECK[39] and the validation menu available in Coot. The first two residues at the N terminus could not be modeled, presumably due to disorder. A summary of the data collection and refinement statistics for four structures are given in Table 1.

pfSPDS inhibition by AdoDATO

To test the inhibitory effect of AdoDATO on the plasmodial enzyme, pfSPDS was cloned, expressed and purified according to Haider *et al.*[19] The activity was measured as described by *Haider et al.* and *Dufe et al.* with the modification of using lower substrate concentrations of 50 μM putrescine and 25 μM dcAdoMet.[19,25] AdoDATO was added in the following concentrations: 0, 1, 5, 10, 20, 50 and 100 μM.

Protein Data Bank accession numbers

The coordinates for the four structures have been deposited with the Protein Data Bank with accession numbers 2I7C, 2PSS, 2PT6 and 2PT9.

Acknowledgements

We thank the staff of Max II synchrotron for support. This work was supported by the Deutsche Forschungsgemeinschaft (Wa 395/10/15). S. Al-Karadaghi is supported by a grant from FLÄK (Forskarskolan i läkemedelsvetenskap). The authors are grateful to Prof. Keijiro Samejima for kindly providing dcAdoMet and 4MCHA.

References

1. Assaraf, Y. G., bu-Elheiga, L., Spira, D. T., Desser, H. & Bachrach, U. (1987). Effect of polyamine depletion on macromolecular synthesis of the malarial parasite, Plasmodium falciparum, cultured in human erythrocytes. *Biochem. J.* **242**, 221–226.
2. Cohen, S. (1998). *A Guide to Polyamines,* Oxford University Press, Oxford, UK.
3. Tabor, C. W. & Tabor, H. (1984). Polyamines. *Annu. Rev. Biochem.* **53**, 749–790.
4. Jiang, Y., Roberts, S. C., Jardim, A., Carter, N. S., Shih, S., Ariyanayagam, M. *et al.* (1999). Ornithine decarboxylase gene deletion mutants of Leishmania donovani. *J. Biol. Chem.* **274**, 3781–3788.
5. Heby, O., Roberts, S. C. & Ullman, B. (2003). Polyamine biosynthetic enzymes as drug targets in parasitic protozoa. *Biochem. Soc. Trans.* **31**, 415–419.
6. Muller, S., Wittich, R. M. & Walter, R. D. (1988). The polyamine metabolism of filarial worms as chemotherapeutic target. *Adv. Exp. Med. Biol.* **250**, 737–743.
7. Muller, S., Coombs, G. H. & Walter, R. D. (2001). Targeting polyamines of parasitic protozoa in chemotherapy. *Trends Parasitol.* **17**, 242–249.
8. Phillips, M. A., Coffino, P. & Wang, C. C. (1987). Cloning and sequencing of the ornithine decarboxylase gene from Trypanosoma brucei. Implications for enzyme turnover and selective difluoromethylornithine inhibition. *J. Biol. Chem.* **262**, 8721–8727.
9. Phillips, M. A. & Wang, C. C. (1987). A Trypanosoma brucei mutant resistant to alpha-difluoromethylornithine. *Mol. Biochem. Parasitol.* **22**, 9–17.
10. Wang, C. C. (1995). Molecular mechanisms and therapeutic approaches to the treatment of African trypanosomiasis. *Annu. Rev. Pharmacol. Toxicol.* **35**, 93–127.
11. Bitonti, A. J., McCann, P. P. & Sjoerdsma, A. (1987). *Plasmodium falciparum* and *Plasmodium berghei*: effects of ornithine decarboxylase inhibitors on erythrocytic schizogony. *Exp. Parasitol.* **64**, 237–243.
12. Bitonti, A. J., Dumont, J. A., Bush, T. L., Edwards, M. L., Stemerick, D. M., McCann, P. P. & Sjoerdsma, A. (1989). Bis(benzyl)polyamine analogs inhibit the growth of chloroquine-resistant human malaria parasites (*Plasmodium falciparum*) in vitro and in combination with alpha-difluoromethylornithine cure murine malaria. *Proc. Natl Acad. Sci. USA*, **86**, 651–655.
13. Kaur, K., Emmett, K., McCann, P. P., Sjoerdsma, A. & Ullman, B. (1986). Effects of dl-alpha-difluoromethylornithine on *Leishmania donovani* promastigotes. *J. Protozool.* **33**, 518–521.
14. Ikeguchi, Y., Bewley, M. C. & Pegg, A. E. (2006). Aminopropyltransferases: function, structure and genetics. *J. Biochem. (Tokyo)*, **139**, 1–9.
15. Pegg, A. E., Poulin, R. & Coward, J. K. (1995). Use of aminopropyltransferase inhibitors and of non-metabolizable analogs to study polyamine regulation and function. *Int. J. Biochem. Cell Biol.* **27**, 425–442.
16. Roberts, S. C., Jiang, Y., Jardim, A., Carter, N. S., Heby, O. & Ullman, B. (2001). Genetic analysis of spermidine synthase from Leishmania donovani. *Mol. Biochem. Parasitol.* **115**, 217–226.
17. Coward, J. K. & Pegg, A. E. (1987). Specific multisubstrate adduct inhibitors of aminopropyltransferases and their effect on polyamine biosynthesis in cultured cells. *Adv. Enzyme Regul.* **26**, 107–113.
18. Shirahata, A., Morohohi, T., Fukai, M., Akatsu, S. & Samejima, K. (1991). Putrescine or spermidine binding site of aminopropyltransferases and competitive inhibitors. *Biochem. Pharmacol.* **41**, 205–212.
19. Haider, N., Eschbach, M. L., Dias, S. S., Gilberger, T. W., Walter, R. D. & Luersen, K. (2005). The spermidine synthase of the malaria parasite Plasmodium falciparum: molecular and biochemical characterisation of the polyamine synthesis enzyme. *Mol. Biochem. Parasitol.* **142**, 224–236.
20. Beppu, T., Shirahata, A., Takahashi, N., Hosoda, H. & Samejima, K. (1995). Specific depletion of spermidine and spermine in HTC cells treated with inhibitors of aminopropyltransferases. *J. Biochem. (Tokyo)*, **117**, 339–345.
21. Shirahata, A., Takahashi, N., Beppu, T., Hosoda, H. & Samejima, K. (1993). Effects of inhibitors of spermidine synthase and spermine synthase on polyamine synthesis in rat tissues. *Biochem. Pharmacol.* **45**, 1897–1903.
22. Byers, T. L., Ganem, B. & Pegg, A. E. (1992). Cytostasis induced in L1210 murine leukaemia cells by the *S*-

adenosyl-l-methionine decarboxylase inhibitor 5′-([(*Z*)-4-amino-2-butenyl]methylamino)-5′-deoxyadenosine may be due to hypusine depletion. *Biochem. J.* **287**, 717–724.
23. Byers, T. L., Wechter, R. S., Hu, R. H. & Pegg, A. E. (1994). Effects of the *S*-adenosylmethionine decarboxylase inhibitor, 5′-([(*Z*)-4-amino-2-butenyl]methylamino)-5′-deoxyadenosine, on cell growth and polyamine metabolism and transport in Chinese hamster ovary cell cultures. *Biochem. J.* **303**, 89–96.
24. Muller, S., Liebau, E., Walter, R. D. & Krauth-Siegel, R. L. (2003). Thiol-based redox metabolism of protozoan parasites. *Trends Parasitol.* **19**, 320–328.
25. Dufe, V. T., Luersen, K., Eschbach, M. L., Haider, N., Karlberg, T., Walter, R. D. & Al-Karadaghi, S. (2005). Cloning, expression, characterisation and three-dimensional structure determination of Caenorhabditis elegans spermidine synthase. *FEBS Letters*, **579**, 6037–6043.
26. Korolev, S., Ikeguchi, Y., Skarina, T., Beasley, S., Arrowsmith, C., Edwards, A. *et al.* (2002). The crystal structure of spermidine synthase with a multisubstrate adduct inhibitor. *Nat. Struct. Biol.* **9**, 27–31.
27. Lu, P. K., Chien, S. Y., Tsai, J. Y., Fong, C. T., Lee, M. J., Huang, H. & Sun, Y. J. (2004). Crystallization and preliminary X-ray diffraction analysis of spermidine synthase from Helicobacter pylori. *Acta Crystallogr. sect. D*, **60**, 2067–2069.
28. Vedadi, M., Lew, J., Artz, J., Amani, M., Zhao, Y., Dong, A. *et al.* (2007). Genome-scale protein expression and structural biology of Plasmodium falciparum and related Apicomplexan organisms. *Mol. Biochem. Parasitol.* **151**, 100–110.
29. Burger, P. B., Birkholtz, L. M., Joubert, F., Haider, N., Walter, R. D. & Louw, A. I. (2007). Structural and mechanistic insights into the action of Plasmodium falciparum spermidine synthase. *Bioorg. Med. Chem.* **15**, 1628–1637.
30. Bowman, W. H., Tabor, C. W. & Tabor, H. (1973). Spermidine biosynthesis. Purification and properties of propylamine transferase from Escherichia coli. *J. Biol. Chem.* **248**, 2480–2486.
31. Sang, O. Y., Yong, S. L., Sung, H. L. & Young, D. C. (2000). Polyamine synthesis in plants: isolation and characterization of spermidine synthase from soybean (*Glycine max*) axes. *Biochim. Biophys. Acta*, **1475**, 17–26.
32. Zappia, V., Cacciapuoti, G., Pontoni, G. & Oliva, A. (1980). Mechanism of propylamine-transfer reactions. Kinetic and inhibition studies on spermidine synthase from Escherichia coli. *J. Biol. Chem.* **255**, 7276–7280.
33. Kabsch, W. J. (1993). Automatic processing of rotation diffraction data from crystals of initially unknown symmetry and cell constants. *J. Appl. Crystallogr.* **26**, 795–800.
34. French, G. S. & Wilson, K. S. (1978). On the treatment of negative intensity observations. *Acta Cryst.*, 517–525.
35. McCoy, A. J., Grosse-Kunstleve, R. W., Storoni, L. C. & Read, R. J. (2005). Likelihood-enhanced fast translation functions. *Acta Crystallogr. sect. D*, **61**, 458–464.
36. Emsley, P. & Cowtan, K. (2004). Coot: model-building tools for molecular graphics. *Acta Crystallogr. sect. D*, **60**, 2126–2132.
37. Murshudov, G. N., Vagin, A. A. & Dodson, E. J. (1997). Refinement of macromolecular structures by the maximum-likelihood method. *Acta Crystallogr. sect. D*, **53**, 240–255.
38. Schuttelkopf, A. W. & van Aalten, D. M. (2004). PRODRG: a tool for high-throughput crystallography of protein–ligand complexes. *Acta Crystallogr. sect. D*, **60**, 1355–1363.
39. Laskowski, R. A., MacArthur, M. W., Moss, D. S. & Thorton, J. M. (1993). PROCHECK: a program to check the stereochemical quality of protein structures. *J. Appl. Crystallogr.* **26**, 283–291.
40. DeLano, W. L. (2002). *The PyMOL Molecular Graphics System*, DeLano Scientific, San Carlos, CA.